Shear characteristics of rectangular Lean Duplex Stainless Steel (LDSS) tubular beams – a finite element study

Sonu J.K[1], Konjengbam Darunkumar Singh[2]

PhD Scholar, Indian Institute of Technology Guwahati, India[1]

Associate Professor, Indian Institute of Technology Guwahati, India[2]

Abstract: This paper reports a numerical study of the shear behavior of Lean Duplex Stainless Steel (LDSS) hollow beams subjected to three point loading. The parameters considered to determine the shear capacity of present finite element model were web thickness of 2-30 mm and ratios of flange thickness to web thickness in the range of 2-5 for each web thickness. Based on the FE analyses, it has been observed that the ultimate shear strength and ductility of hollow sections increased with decreasing web height/thickness ratio (h_w/t_w) and increasing flange thickness / web thickness ratio (t_f/t_w). In comparison to EN 1993-1-4 (2006), FE predicted slightly higher values of ultimate shear, with good agreement on the overall behavior of ultimate load with variation in h_w/t_w, indicating the applicability of the present EN 1993-1-4 (2006) on the shear design of LDSS rectangular hollow steel. However, the predictions by FE on shear buckling reduction factor showed higher values (~ 20-140% higher) that those predicted by EN 1993-1-4 (2006).

Keywords: Hollow steel Beam, shear behavior, LDSS, Abaqus.

I.   INTRODUCTION

Many of the researches and construction industry applications of steel members are generally overshadowed by carbon steel due to comparatively lower cost, long experience, applicable design rules and a large variety of strength classes; however carbon steel suffers inherently from relatively low corrosion resistance and higher material cost. But in contrast to carbon steel, a variety of stainless steel types can provide a very wide collection of mechanical properties and material features to suit the demands of several and diverse engineering applications, along with the benefits of high corrosion resistance, high strength, smooth and uniform surface, aesthetic appearance, good ductility, impact resistance and ease of maintenance and construction. These benefits have inspired a moderately upturn in the use of stainless steel in construction industry in the recent years. Traditionally, in the constructional industry, austenitic steel grades are used visibly, however, with ever increasing nickel prices (nickel content of ~ 8% -11% in austenitic stainless steel) there is an stepping up in the demand for lean duplex stainless steel (LDSS) with low nickel content of ~ 1.5%, such as grade EN 1.4162 (Gardner, 2005, Badoo, 2008, EN 10088-4, 2009) LDSS grade EN 1.4162 in specific, with twice the mechanical strength of traditional austenitic and ferritic stainless steel has a future in construction industry, and large growth and progress has taken place in its use over the last 20 years or so. The demand for LDSS owes to rising raw material costs, such as nickel, along with raising demand for improved corrosion resistance, high temperature properties, adequate weldability, strength and fracture toughness, facilitating a reduction in section sizes leading to higher strength to weight ratios (e.g. The of anous and Gardner, 2009, Hassanein, 2011, Patton and Singh, 2012). LDSS is now included in the material standard EN 10088-4 (2009), however, it is not currently covered by any other structural design code, due to the lack of sufficient information on structural characteristics (Saliba and Gardner, 2013). As a result, in the recent years, several researchers (Hassanein, 2010, Theofanous

and Gardner, 2010, Huang and Young, 2012) have started showing increasing interests in a broad programme of experimental and numerical testing of LDSS structural members such as beams (e.g. square (Theofanous and Gardner, 2010), columns (e.g. rectangular (Theofanous and Gardner, 2009, Huang and Young, 2013), circular (Umbarkar et. al, 2013), non-rectangular (Patton and Singh, 2012.)), to investigate their structural performances. In addition to the various closed sections (i.e. tubular), investigations have also been reported for I-sections (Huang and Young, 2013, Saliba and Gardner, 2013, Hassanein, 2011, 2013). However, to the best of our knowledge, no reported study has been made on the shear response of tubular beams made of LDSS. Hence an effort has been made to explore the structural behavior (especially shear capacity) of hollow LDSS tubular beams, in this paper. Based on the results generated through finite element modeling, applicability of the present provisions of Eurocode 3: Part 1-4 (2006) for stainless steel hollow beams subjected to shear is checked.

II.   NUMERICAL MODELING THROUGH ABAQUS

The numerical modeling approach followed in this research is similar to the method described by Estrada et. al., (2008), Theofanous and Gardner (2010), Saliba and Gardner (2013). Geometry of the analyzed beam is shown in Fig. 1, where L, h_w, b_f, and t_f are the length, height of the web, breadth of the flange, and flange thickness respectively. The in-plane cross-sections were constrained at the both ends and midspan of the beam to restrain buckling at those locations using kinematic coupling (see e.g. Theofanous and Gardner, 2010) available in Abaqus (2010). The finite element type used for the analysis is the four-noded general purpose shell element with reduced integration (S4R) which is known to provide accurate results for thin-walled members (e.g. Theofanous and Gardner, 2009, Saliba and Gardner, 2013, Patton and Singh, 2012, 2013) as shown in Fig.2.

In order to provide constant shear along the span, the analyzed beams were simply supported at the ends and point load is applied at the mid-span of the beam. Loading and end support conditions were applied through the reference points, RP1, RP2 and RP3, which were tied

with the periphery cross-sectional nodes, at the mid span and both ends of the cross-section of beam respectively (see Fig. 3). The load is then applied at RP2 to transfer uniform load to flanges and webs of the coupled cross section.
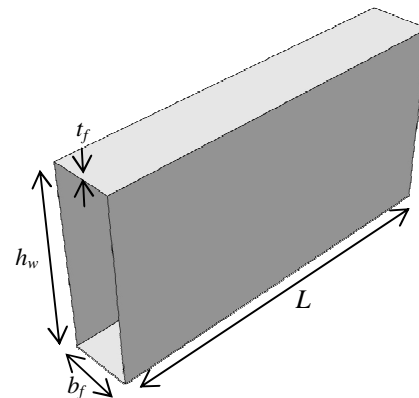
Fig. 1. Schematic diagram of FE LDSS hollow beam.

(a)   (b)
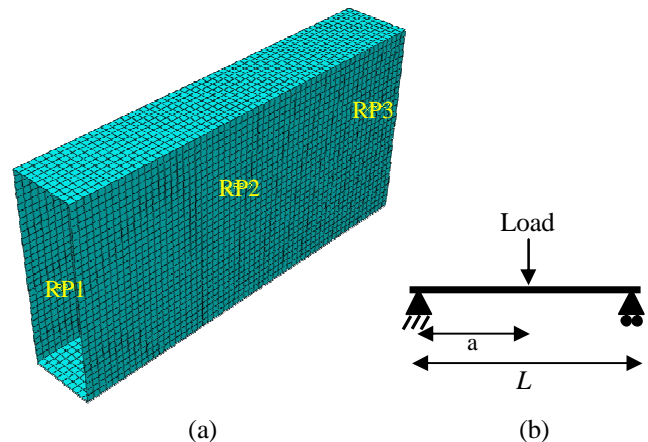
Fig. 2. a) FE mesh (RP1, RP2 and RP3 are reference points b) boundary condition.
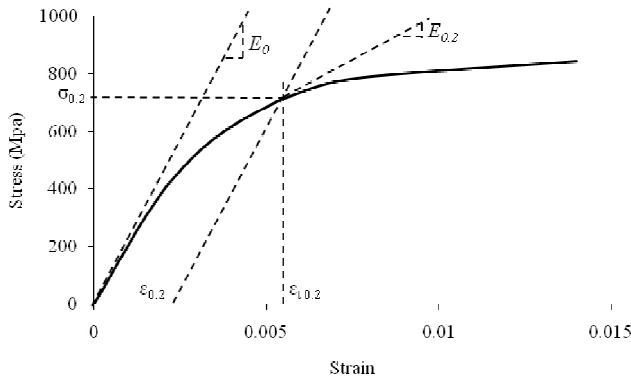
Fig. 3. Schematic diagram of stress-strain curve of LDSS material Grade EN 1.4162 (Gardner & Ashraf, 2006).

Local geometric imperfections were incorporated in to the FE model after conducting eigen-value analysis (Gardner, 2002). Lowest eigen-mode was served as the initial imperfection of the actual structure. The imperfection amplitude given to the FE model was based on the proposal by Gardener and Nethercot (2004) for stainless steel, which is the modified model of Dawson and Walker (1972).

Ramberg-Osgood (1943) model gives a good prediction of experimental data up to proof stress ($\sigma_{0.2}$), but it over estimates the stresses beyond this limit at higher strains. Therefore a modified Ramber-Osgood model (or compound R-O model) for higher stresses ($> \sigma_{0.2}$) as suggested by Rassmussen (2003) and Gardner (2002) were used. The material data (specimen data used for validation) used for the analysis is taken from the experiment conducted by Theofanous and Gardner (2010) as shown in Table 1. Weighted average compressive and tensile material properties were assigned to the compressive and tensile regions of the model. Poisson's ratio was taken as 0.3. Fig. 3 shows the schematic stress-strain curve of LDSS material Grade EN 1.4162 which is used as input to the FE model after converted to true stress (σ_{true}) and true plastic strains $\left(\varepsilon_{true}^{pl} \right)$ values using the following Eqs. 1 & 2.

$$\sigma_{true} = \sigma_{norm} \left(1 + \varepsilon_{norm} \right) \qquad (1)$$

$$\varepsilon_{true}^{pl} = ln\left(1 + \varepsilon_{norm}\right) - \frac{\sigma_{true}}{E_0} \qquad (2)$$

where σ_{norm} and ε_{norm} are engineering stress and strain.

Table 1
a) Tensile and b) compressive flat material properties of SHS- 60x60x3 (Theofanous and Gardner, 2010)

Material Property	E (MPa)	$\sigma_{0.2}$ (MPa)	$\sigma_{1.0}$ (MPa)	σ_u (MPa)	Compound R-O coefficients	
					n	$n'_{0.2,0.1}$
Tension	209797	755	819	839	6.0	4.3
Compression	206430	711	845		5.0	2.7

III. VERIFICATION OF FINITE ELEMENT MODEL

An experimental investigation on LDSS (Grade EN 1.4162) hollow beam conducted by Theofanous and Gardner (2010) was used to validate the method of FE modeling followed in the present study. In addition to the above mentioned (in numerical modeling) material properties assigned to flat portions of the specimen, tensile corner properties were assigned to the corner regions. Table 2 shows the LDSS square beam outer dimensions of the tested specimen.

Table 2
Beam dimension (Theofanous and Gardner, 2010)

Specimen	L (mm)	B (mm)	D (mm)	t (mm)	r_i (mm)
SHS-60x60x3-B2	1100	60	60	3.10	2.3

L = Length, B = Width, H = Depth, t = thickness, r_i = internal corner radius

Fig. 4 shows a comparison of experimental (Theofanous & Gardner, 2010) and present FE plot of moment-rotation variation. A good agreement can be seen between experimental and FE results in terms of the overall behavior, in addition to the specific values of the ultimate moment capacity (M_u) and rotation θ_u at M_u. The verification showed the method followed for FE modeling is capable to simulate the structural behavior of rectangular hollow steel beams.
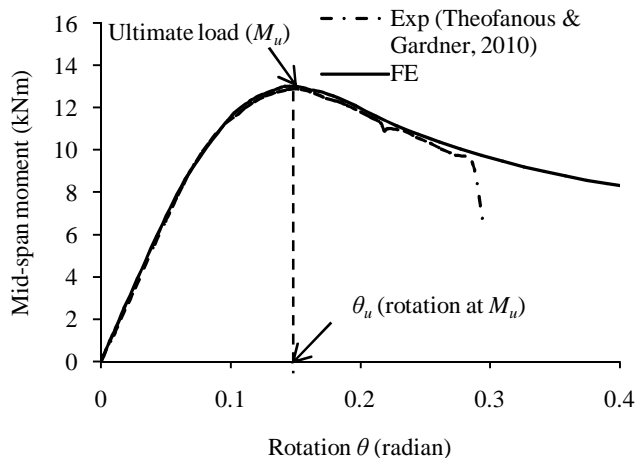
Fig. 4. Variation of mid-span moment vs rotation (SHS-60 x 60 x 3-B2).

IV. PARAMETRIC STUDY OF HOLLOW STEEL BEAMS

To understand the shear response of rectangular hollow (LDSS) beam, FE analysis was conducted to get the FE ultimate shear capacity ($V_{u, FE}$), mid-span deflection and deformation patterns. Parameters considered for the analysis of beams were various ratios of flange thickness/web thickness (t_f/t_w = 2-5) for web thickness (t_w) of 2-30 mm. Span (L) of the beam, flange width (b_f) and shear span/web depth (a/h_w) are 1200 mm, 200 mm and 1.0 respectively. The shear span (a) is then equal to L/2 = 600mm. Beams were designated using labels such as W600BF200TF4TW2 where W600, BF200, TF4, TW2 denotes web depth of 600 mm, flange width of 200 mm, flange thickness of 4 mm and web thickness of 2 mm respectively.

V. RESULTS AND DISCUSSION

Variations of shear load (V) with mid-span displacement (δ) and normalized section capacity, V_u/V_y vs δ, (V_u is the ultimate shear capacity and V_y is the yield shear capacity given by ($f_y/\sqrt{3}$) ($2t_w h_w$), where f_y = yield stress) have

been plotted as shown in Figs 5a & b by varying flange thickness (t_f/t_w= 2-5 keeping t_w = 2). It can be seen from Fig. 5a that V_u increases with increasing t_f, and further decreasing sharpness of the curve at V_u for increasing t_f can also be seen. Deformation at V_u (i.e. δ_u) is also found to increase with increasing t_f . From Fig. 5b, it is observed that for all the flange thicknesses that have been considered, V_u is much lesser than the yield shear capacity of the sections i.e. $V_u/V_y < 1$. It may be noted that V_y is calculated based on the yield capacity of the web without considering the effect of the shear capacity of the web. The ratio $V_u/V_y < 1$ indicates that the section has buckled prior to yielding of the web (caused by the local buckling of slender web). Thus it can be seen that although the shear carrying capacity of the section is controlled by web, V_u and δ_u can be significantly improved by increasing the thickness of the flange. For slender web it can be observed that, an increase of 150 % in flange thickness led to about 45 % increase in V_u. The appearance of the plateau region of the V vs δ near the ultimate shear load may related to the enhance load distribution and resistance of the flange, resulting in the delay of the formation of plastic hinges on the flange, as a result of increasing its thickness. Fig. 6 shows the variation of V_u/V_y with δ for increasing web thickness (t_w) from 2 – 30 mm, keeping t_f/t_w = 5. Thus it can be seen from Fig. 6 that for $t_w > 8$ mm, $V_u/V_y > 1$, suggesting that as the web has become more stocky, the value of V_u has shown considerably higher, with extended plateau of the V vs δ profile.

Figs. 7 a & b show the variation of V_u and V_u/V_y with h_w/t_w for various values flange thickness (t_f/t_w = 2-5). It can be seen from Fig. 7a that shear capacity drops asymptotically as the value of h_w/t_w is increased from 20 to 100, and flattens out for $h_w/t_w > 100$, consistent with the increasing slenderness of the web. It can also be observed that increase in t_f/t_w from 2 to 5, had minor effect on V_u for larger values of h_w/t_w (>100), but increased values of V_u for increasing values of t_f/t_w for $h_w/t_w < 100$. From Fig. 7b, it can be seen that, for $h_w/t_w < 100$, $V_u/V_y > 1$, whilst it is $V_u/V_y < 1$, for $h_w/t_w > 100$, indicating that lower values of h_w, prompt the cross-section to yield (and hence better mobilization of the stress) prior to reaching V_u, and this improves with increasing flange thickness.

Present FE results are used to assess the validity of shear resistance model in EN 1993-1-4 (2006) to LDSS

rectangular hollow sections. The ultimate shear force obtained from FE has been compared to the unfactored design shear resistance using EN 1993-1-4 (2006) in Fig. 8 for $t_f/t_w = 5$. It can be seen from Fig 8 that overall behavior of the variation of V_u with h_w/t_w between FE and EN 1993-1-4 (2006) matches well. Table 3 shows the comparison of FE and EN 1993-1-4 (2006) for $t_f/t_w = 2$-5 and $a/h_w = 1$. It can be observed that the FE values are in close agreement with the EN 1993-1-4 (2006) predicted values for ultimate shear capacity, with a mean of 1.10 and COV of 0.05. It shows that the present EN 1993-1-4 (2006) design rules for stainless steel may be applied to the LDSS hollow steel beams.

Fig. 9 shows the contribution of web in shear resistance mechanism of beam ($t_f/t_w = 5$) in terms of shear buckling reduction factor (χ_w) against web slenderness $\bar{\lambda}_w$ (χ_w and $\bar{\lambda}_w$ are defined in Appendix). FE results have been plotted by subtracting the flange contribution in shear from the ultimate shear and the resultant values have been normalized by the yield capacity of web in shear. Variation of von-Mises stress superimposed over deformed shapes at ultimate shear load are also plotted both at low and high values of $\bar{\lambda}_w$ as shown in Fig. 9. A high value of $\bar{\lambda}_w$ indicates slender web section. It is evident from Fig. 9 that higher the values of slenderness give less contribution (indicated by lower value of χ_w) of the web panel to the whole shear resistance mechanism. EN-1993-1-4 gives design of stainless steel plates loaded in shear, although it is conservative (FE predicted 20-140 % higher values of χ_w) for the design of rectangular hollow sections. The values above 1.2 at low slenderness show the sections undergone strain hardening (e.g. Saliba, 2013). From the inset deformed shapes it can be seen that the failure mode corresponding to slender web section (e.g. at $\bar{\lambda}_w = 4.60$) is predominantly through local shear buckling of the web along with formation of plastic hinges near the supports. However, when the web becomes stocky (e.g. at $\bar{\lambda}_w = 0.31$), the failure mode is predominately bending in nature. Stocky webs are able to support higher load without any signs of local diagonal buckling as observed for slender webs. This results in the

appearance of plastic hinge at the mid span, and buckling of the top flange.

(a)

(b)
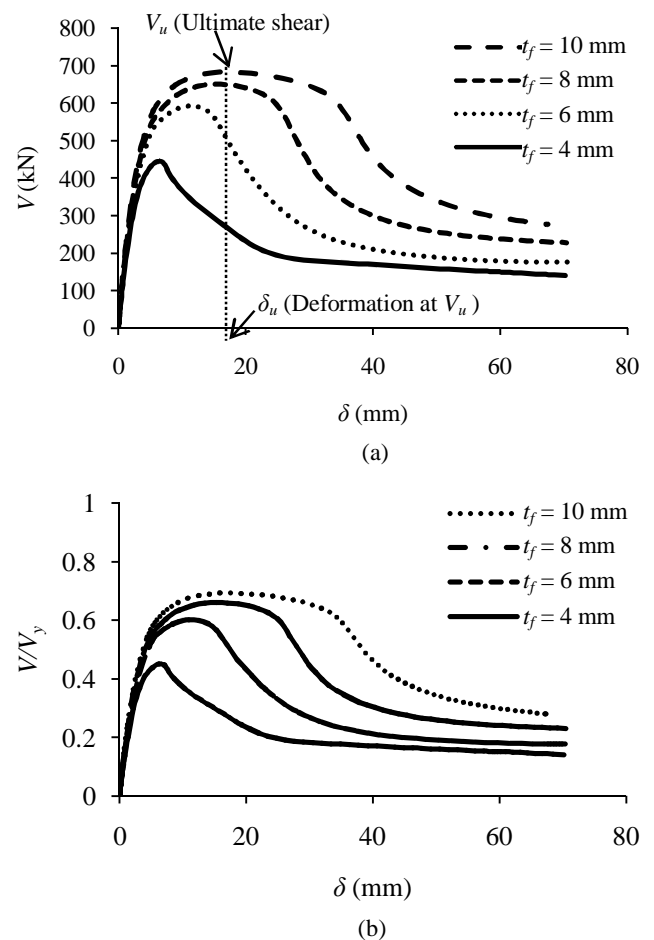
Fig. 5. Variation of a) V vs δ and (b) V/V_y vs δ (t_w=2 mm).

t_w = 30 mm
t_w = 20 mm
t_w = 8 mm
t_w = 4 mm
t_w = 2 mm
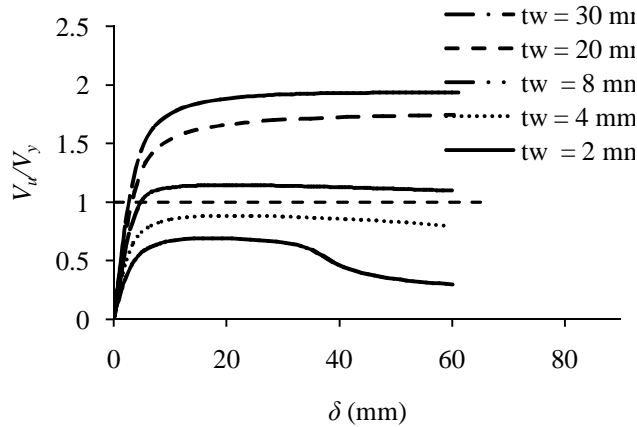
Fig. 6. Variation of V vs δ curve (t_f/t_w = 5).

(b)
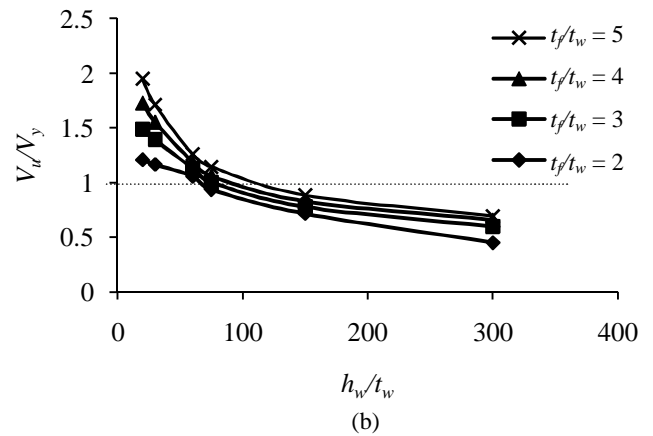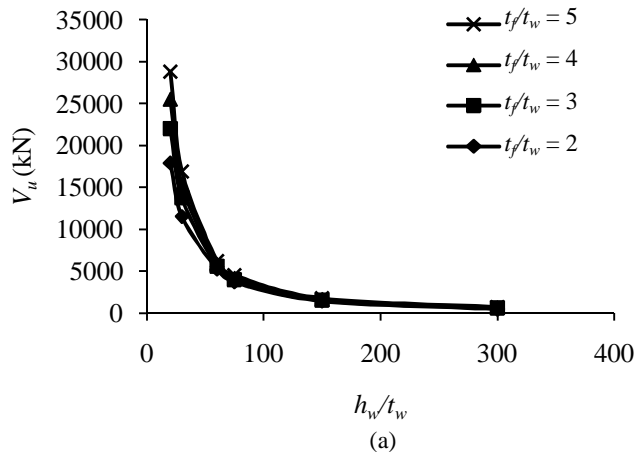
Fig. 7. Variation of a) V_u vs h_w/t_w and (b) V_u/V_y vs h_w/t_w (t_w = 2 mm).

(a)
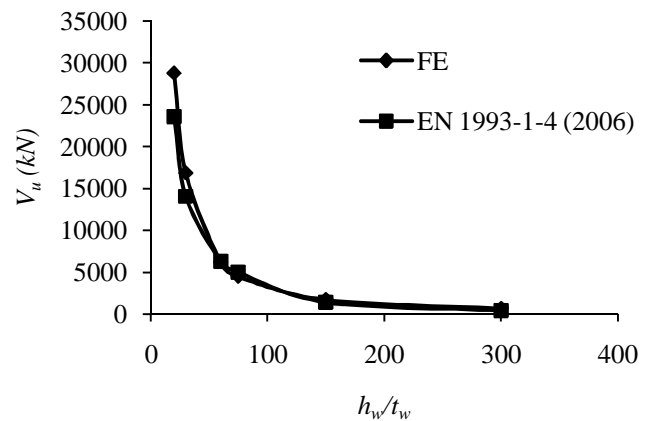
Fig. 8. Comparison of EN 1993-1-4 (2006) and FE results for vs h_w/t_w (t_f/t_w = 5).

Table 3. Comparison of FE results with EN 1993-1-4 (2006) for t_f/t_w (2-5) of a/h_w = 1.

Specimens	$V_{u,FE}/V_{EN\,1993-1-}$
W600BF200TF4TW2	1.22
W600BF200TF8TW4	1.12
W600BF200TF16TW8	0.80
W600BF200TF20TW10	0.91
W600BF200TF40TW20	0.96
W600BF200TF60TW30	0.95
W600BF200TF6TW2	1.54
W600BF200TF12TW4	1.16

![IJIRSET logo]

ISSN (Online) : 2319 - 8753
ISSN (Print)   : 2347 - 6710

International Journal of Innovative Research in Science, Engineering and Technology

An ISO 3297: 2007 Certified Organization   Volume 3, Special Issue 4, March 2014

National Conference on Recent Advances in Civil Engineering (NCRACE-2013)

During 15-16 November, 2013

Organized by

Department of Civil Engineering, North Eastern Regional Institute of Science and Technology, Nirjuli, Itanagar, Arunachal Pradesh, India.

W600BF200TF24TW8	0.83
W600BF200TF30TW10	0.93
W600BF200TF60TW20	1.09
W600BF200TF90TW30	1.17
W600BF200TF8TW2	1.60
W600BF200TF16TW4	1.19
W600BF200TF32TW8	0.85
W600BF200TF40TW10	0.95
W600BF200TF80TW20	1.17
W600BF200TF120TW30	1.22
W600BF200TF10TW2	1.60
W600BF200TF20TW4	1.22
W600BF200TF40TW8	0.90
W600BF200TF50TW10	0.99
W600BF200TF100TW20	1.20
W600BF200TF150TW30	1.22
Mean	1.10
COV	0.05

1) The ultimate shear strength and ductility of hollow sections increased with decreasing h_w/t_w and increasing t_f/t_w.

2) In comparison to EN 1993-1-4 (2006), FE predicted slightly higher values of ultimate shear, with good agreement on the overall behavior of ultimate load with variation in h_w/t_w, indicating the applicability of the present EN 1993-1-4 (2006) on the shear design of LDSS rectangular hollow steel. However, the predictions by FE on shear buckling reduction factor showed higher values (~ 20-140% higher) that those predicted by EN 1993-1-4 (2006).

3) FE results also showed that at higher values of $\bar{\lambda}_w$, the failure mode is predominately controlled by diagonal local shear buckling of the web (with the formation of plastic hinges near the supports), whiles for lower values of $\bar{\lambda}_w$, it is predominately in bending mode (with the formation of plastic hinge near the midspan or load location).

Fig. 9. Variation of χ_w with $\bar{\lambda}_w$ ($t_f/t_w = 5$).

VI.   CONCLUSIONS

This paper presents FE study of shear behavior of LDSS (Lean Duplex Stainless Steel) rectangular hollow steel beams using Abaqus (2010) by varying cross sectional parameters like flange thickness and web thickness to estimate the shear capacity and the mode of failures. Based on the study following conclusions are made:

Appendix

Shear buckling reduction factor (χ_w) (EN 1993-1-4 (2006))

$$\chi_w = \eta \qquad\qquad \text{for } \bar{\lambda}_w \leq \frac{0.6}{\eta}$$

$$\chi_w = 0.11 + \frac{0.64}{\bar{\lambda}_w} - \frac{0.05}{\bar{\lambda}_w{}^2} \qquad\qquad \text{for } \bar{\lambda}_w > \frac{0.6}{\eta}$$

The slenderness parameter, $\bar{\lambda}_w = \dfrac{b_w}{37.4 * t * \varepsilon * \sqrt{k_\tau}}$

b_w = clear distance between flanges, t = thickness of plate

$$\eta = 1.2, \quad \varepsilon = \left[\frac{235}{f_y}\frac{E}{210000}\right]^{0.5}$$

E = Young's modulus, f_y = yield stress,

k_τ = Shear buckling co-efficient (EN 1993-1-5(2001))

$$k_\tau = 5.34 + 4.00\left(\frac{b}{a}\right)^2 \text{ when } a/b \geq 1$$

$$k_\tau = 4.00 + 5.34\left(\frac{b}{a}\right)^2 \text{ when } a/b < 1$$

a is the distance between the support and loading

b is the width of the plate (for web the clear distance between flanges h_w)

REFERENCES

[1] Abaqus. Abaqus/Standard user's manual volumes I-III and ABAQUS CAE manual. Version 6.9-EF1, Dassault Systems Corp., Providence, USA. 2010.

[2] Baddoo NR. Stainless steel in construction: a review of research, applications, challenges and opportunities. J Construct Steel Res 2008; 64: 1199-1206.

[3] Dawson RG, Walker AC. Post-buckling of geometrically imperfect plates. Journal of the Structural Division, ASCE 1972; 98:ST1:75-94.

[4] EN 10088-4. Stainless steels. Part 4: technical delivery conditions for sheet/plate and strip of corrosion resisting steels for general purposes. CEN; 2009.

[5] ENV 1993-1-4. Eurocode 3: design of steel structures. Part 1.4: general rules – supplementary rules for stainless steels. CEN; 1996.

[6] Estrada I, Real E and Mirambell E. Shear resistance in stainless steel plate girders with transverse and longitudinal stiffening, Jouranal of Constructional Steel Research 2008; 64: 1239-1254.

[7] Gardner L. A new approach to structural stainless steel design. PhD Thesis. Structures Section, Dept of Civil and Ernvironmental Engineering. Imperial College London, UK. 2002.

[8] Gardner L, Nethercot DA. Numerical modeling of stainless steel structural components-A consistent approach. Journal of Structural Engineering, ASCE 2004; 130(10):1586-601.

[9] Gardner L. The use of stainless steel in structures. Prog Struct Eng mater 2005; 7(2): 45-55.

[10] Gardner L, Ashraf M, Strucural design for non-linear metallic materials. Enginnering Structures 2006; 28(6): 926-34.

[11] Hassanein MF & Kharoob OF., Shear strength of transversly stiffened tubular flange plate girders, Eng Struct. 2010; 32: 2617-2630.

[12] Hassanein MF, Finite element investigation of shear failure of lean duplex stainless steel plate girders, Thin-Walled Structures 49 (2011) 964–973.

[13] Hassanein MF, Silvestre. Flexural behavior of lean duplex stainless steel girders with slender unstiffened webs, J of Const Steel Res 85 (2013) 12–23.

[14] Huang Y and Young B. Material properties of cold-formed lean duplex stainless steel sections. Thin Wall Struct 2012; 54:72–81.

[15] Huang Y and Young B, Experimental and numerical investigation of cold-formed lean duplex stainless steel flexural members, Thin-Walled Structures 2013: 73:216–228.

[16] Patton ML. and Singh KD. Numerical modeling of lean duplex stainless steel hollow columns of square, L-, T-,and +-shaped cross sections under pure axial compression. Thin-Walled Structures 2012: 53:1–8.

[17] Patton ML and Sing KD. Buckling of fixed-ended lean duplex stainless steel hollow columns of square, L-, T-, and + -shaped sections under pure axial compression- a finite element study. Thin-Walled Structures 2013: 63:106–116.

[18] Ramberg W.,Osgood W.R. Description of stress–strain curves by three parameters. Technical Note No 902, Washington, DC: National advisory committee for aeronautics 1943.

[19] Rasmussen KJR. Full-range stress-strain curves for stainless steel alloys. Journal of Constructional steel research 2003; 59: 47-61.

[20] Saliba N and Gardner L, Cross-section stability of lean duplex stainless steel welded I-sections, J Constr Steel Res 80 (2013) 1-14.

[21] Saliba N, Gardner L. Experimental study of the shear response of lean duplex stainless steel plate girders. Eng Struct 2013; 46: 375–391.

[22] Saliba N, Gardner L. Experimental study of the shear response of lean duplex stainless steel plate girders. Eng Struct 2013; 46: 375–391.

[23] Theofanous M, Gardner L. Testing and numerical modelling of lean duplex stainless steel hollow section columns. Eng Struct 2009;31(12):3047–58.

[24] Theofanous M, Gardner L. Experimental and numerical studies of lean duplex stainless steel beams. J Constr Steel Res 2010;66:816-25.

[25] Umbarkar KR, Patton ML. and Singh KD. Effect of single circular perforation in lean duplex stainless steel (LDSS) hollow circular stub columns under pure axial compression. Thin-walled Structures 2013: 68: 18-25.